◆ Human Brain Mapping 35:5486–5499 (2014) ◆

Processing of Nociceptive Input From Posterior to Anterior Insula in Humans

Maud Frot,[1,2]* Isabelle Faillenot,[1,3] and François Mauguière[1,2,4]

[1]*INSERM, U1028, Central Integration of Pain Unit, Neuroscience Research Center, Bron F-69677, France*
[2]*Claude Bernard University Lyon 1, Lyon F-69000, France*
[3]*Department of Neurology, University Hospital, Saint-Etienne Cedex 2, F-42055, France*
[4]*CHU Lyon, Functional Neurology and Epilepsy Department, Neurological Hospital, Bron F-69677, France*

Abstract: Previous brain imaging studies have shown robust activations in the insula during nociceptive stimulation. Most activations involve the posterior insular cortex but they can cover all insular gyri in some fMRI studies. However, little is known about the timing of activations across the different insular sub-regions. We report on the distribution of intracerebrally recorded nociceptive laser evoked potentials (LEPs) acquired from the full extent of the insula in 44 epileptic patients. Our study shows that both posterior and anterior subdivisions of the insular cortex respond to a nociceptive heat stimulus within a 200–400 ms latency range. This nociceptive cortical potential occurs firstly, and is larger, in the posterior granular insular cortex. The presence of phase reversals in LEP components in both posterior and anterior insular regions suggests activation of distinct, presumably functionally separate, sources in the posterior and anterior parts of the insula. Our results suggest that nociceptive input is first processed in the posterior insula, where it is known to be coded in terms of intensity and anatomical location, and then conveyed to the anterior insula, where the emotional reaction to pain is elaborated. *Hum Brain Mapp 35:5486–5499, 2014.* © **2014 Wiley Periodicals, Inc.**

Key words: insula; pain; laser-evoked potentials; intracerebral recordings; humans

INTRODUCTION

The insula is a hidden region of the brain, deeply buried behind the frontal, parietal, and temporal opercula. In the last decades, a large number of studies have shown that, in spite of its small size (less than 2% of the total cortical surface area, Nieuwenhuys, 2012), the insula is a very complex region. It is involved in a multitude of functions from sensorimotor to cognitive and social-emotional processes, as reviewed in a recent voxel-based meta-analysis of neuroimaging data [Kurth et al., 2010a]. This functional complexity mirrors an anatomical sophistication recently illustrated by the identification of seven distinct cytoarchitectonic areas in the insular cortex [Eickhoff et al., 2006, Kurth et al., 2010b; Morel et al., 2013]. One of the distinct features of sensory, vegetative and emotional inputs processed by the insular cortex is that most of them are of immediate relevance to the organism. In particular, painful stimuli tend to produce the largest bilateral activation of the insular cortex [Kurth et al., 2010a, Mazzola et al., 2012a]. Moreover, lesions of this region in humans can notably modify pain processing by reducing the emotional reaction to pain

Additional Supporting Information may be found in the online version of this article.

*Correspondence to: Maud Frot, Inserm U1028, CRNL, Hôpital Neurologique, 59 Bd. Pinel, 69677 Bron Cedex, France.
E-mail: maud.frot@univ-lyon1.fr

Received for publication 12 November 2013; Revised 27 May 2014; Accepted 27 May 2014.
DOI: 10.1002/hbm.22565
Published online 11 June 2014 in Wiley Online Library (wileyonlinelibrary.com).

[Berthier, 1988; Schnitzler and Ploner, 2000], or by provoking hyperalgesia, central pain or allodynia in association with increased pain sensation threshold and reduced amplitude of LEPs recorded from the scalp [Garcia-Larrea et al., 2010; Moisset and Bouhassira, 2007].

Insular activations during painful stimuli are consistently reported in brain imaging studies [Apkarian et al., 2005; Duerden and Albanese, 2011]. Therefore, the insular cortex is considered to be a major cortical structure involved in pain perception. In particular, the insular cortex participates both in a first-order nociceptive matrix composed of the posterior insula and inner opercular cortex in the upper bank of the Sylvian fissure, and in a second-order perceptual matrix consisting of the mid- and anterior insular cortices, the anterior cingulate gyrus, anterior frontal, and posterior parietal areas, which ensure transition from cortical nociception to conscious pain and its attentional–cognitive modulation [see Garcia-Larrea and Peyron, 2013 for a review]. Thus, if the posterior part of the insula is mainly involved in sensory aspects of pain processing [Brooks et al., 2005; Henderson et al., 2007], the anterior insular cortex is more implicated in affective/emotional aspects of pain and visceral reaction associated to painful sensation [see Duerden and Albanese, 2011; Garcia-Larrea and Peyron, 2013; Schweinhardt and Bushnell, 2010 and for reviews].

Although the spatial resolution of fMRI recordings is fine enough to distinguish between pain activations of posterior and anterior insular cortices, it does not provide accurate information about the timing of activations across these two regions. This issue can be assessed by electrophysiological methods with a time resolution of less than 1 ms. However, if numerous source modeling studies of scalp recorded LEPs converged on the existence of bilateral sources in the operculo-insular region [see Garcia-Larrea et al., 2003 for a review], less than 20% of them have shown LEP sources precisely located in the insular cortex [Apkarian et al., 2005]. This is essentially due to the limited spatial resolution of deep source localization based on modeling of scalp EEG or MEG signals. Therefore, only direct recordings inside the insular cortex offer the possibility of exploring both spatial and temporal aspects of pain processing in this region.

In this study, we report on the distribution of nociceptive LEPs in the insula recorded by means of depth intracerebral electrodes exploring the whole extent of the insular cortex. By using a nociceptive laser stimulation that selectively activates the Aδ peripheral fibers, we explored the early stages and sensory aspects of pain processing in the insula and assessed the time gradient between posterior and anterior insular cortex activation by painful stimuli.

PATIENTS AND METHODS

Patients

Forty patients (20 women and 20 men; mean age 30 years, range, 14–59 years) were included in this study; all of them suffered from focal refractory epileptic seizures originating from the temporal lobe but with a suspected spread to supra-sylvian frontal and/or parietal cortex. Invasive recordings were carried out using stereotactically implanted intra-cerebral electrodes (Stereo-Electro-Encephalography or SEEG) before neurosurgery. In particular, patients included in this study had electrodes implanted in the insular cortex for the recording of their seizures (see Isnard et al., 2000, 2004 for a complete description of the rationale of electrode implantation). Each electrode had 10–15 contacts, each of them 2 mm long, separated by 1.5 mm, and could be left in place chronically up to 15 days. Nineteen patients were implanted in the left hemisphere and 21 in the right hemisphere.

The recording of spontaneous seizures is routinely completed by functional mapping of potentially eloquent cortical areas using evoked potential recordings and cortical electrical stimulation in patients implanted with depth electrodes before epilepsy surgery (for a description of the stimulation procedure see Ostrowsky et al., 2002; Mazzola et al., 2006). In agreement with French regulations relative to invasive investigations with a direct individual benefit, patients gave their consent after being fully informed about electrode implantation, SEEG, evoked potential recordings, and cortical stimulation procedures used to localize the epileptogenic and eloquent cortical areas. The laser stimulation paradigm and LEP recording procedure were approved by the local Ethics Committee.

Evoked potential recordings were performed at the end of the SEEG monitoring period, which lasted a maximum of two weeks. At the time of the SEEG procedure antiepileptic treatment had been tapered down, so that all patients were under therapy with one or two of the major antiepileptic drugs (carbamazepine, phenytoin, valproate, lamotrigine, or topiramate) with daily dosages at, or slightly under, the minimum of their usual therapeutic range.

Electrode Implantation

Intracerebral electrodes were implanted using Talairach's stereotactic frame. As a first step, a cerebral angiography was performed in stereotactic conditions using an X-ray source located 4.85 m away from the patient's head. This eliminates the linear enlargement due to X-ray divergence, so that the films could be used for measurements without any correction. In a second step, the relevant targets were identified on the patient's MRI, previously enlarged to a scale of one-to-one. As MR and angiographic images were at the same scale, they could easily be superimposed. Adapting the planned implantation site to avoid larger vessels, thus minimizes the risk of hemorrhage during electrode implantation.

To check for the final position of each electrode with respect to the targeted anatomical structures, a post-implantation brain MRI was performed in nine patients in

whom nonferromagnetic MRI compatible electrodes were used. In the 31 others (patients implanted before 2010), MRI could not be performed with electrodes in place because of the physical characteristics of the stainless steel contacts. In these cases the scale 1 : 1 post implantation skull radiographs performed within the stereotactic frame of Talairach and Tournoux [1988] were superimposed to the preimplantation scale 1 : 1 MRI slice corresponding to each electrode track, thus permitting to plot each contact onto the appropriate MRI slice of each patient [MRIcro® software; Rorden and Brett, 2000] and determining its Talairach coordinates.

Anatomical scans were acquired on a 3-Tesla Siemens Avanto Scanner using a 3D MPRAGE sequence with following parameters: TI/TR/TE 1100/2040/2.95 ms, voxel size: $1 \times 1 \times 1$ mm^3, FOV = 256×256 mm^2. Enough sagittal slices were acquired for covering the whole brain.

The following image analysis procedure was carried out. MR images were centered on the Anterior Commissure (AC) and oriented in the Talairach and Tournoux reference space. In order to map electrode contacts to standard stereotaxic space (Montreal Neurological Institute, MNI), regions of interest (ROIs) were defined in each subject's native space using the MarsBar toolbox [Brett et al., 2002]. For each insular contact, a ROI was defined as a sphere of 1.5 mm radius centered on the corresponding Talairach coordinate derived from the procedure described in the preceding paragraph. This ROI was saved as an image in the patient space. Using SPM8 (Wellcome Department of Cognitive Neurology), the anatomical image was normalized to the MNI template brain image using the segmentation step [Ashburner and Friston, 2005]. By applying the normalization parameters to the ROI images, MNI coordinates of the spheres could be directly obtained from the images. The 40 anatomical images were then averaged and insular sulci were drawn for illustration.

Insular Recordings

In a given patient, responses recorded in referential and bipolar modes obtained from each contact located in a given insular gyrus were considered. A total of 239 insular sites were explored. Along each electrode track, the contact exhibiting the largest peak-to-peak response in referential mode was selected; this led to a selection of 82 insular contacts, 34 in the left and 48 in the right hemisphere.

The locations of these contacts and their mean stereotactic coordinates are shown in Figure 1 and Table I. The different gyri within the insula were identified considering the morphological aspect of gyral and sulcal structures on the brain MRI of each patient. We thus defined the posterior and anterior parts of the insula as the regions located posterior and anterior to the insular central sulcus, respectively. According to several anatomical studies, this sulcus represents a continuation of the Rolandic fissure on the dorsolateral convexity of the cerebral hemisphere [see Nieuwenhuys, 2012 for a review]. The posterior insula is divided into two long gyri, known as the posterior long gyrus (PLG) and the anterior long gyrus (ALG). The anterior insula is composed of three short gyri, the posterior short gyrus (PSG), the middle short gyrus (MSG) and the anterior short gyrus (ASG) [Naidich et al., 2004; Nieuwenhuys, 2012]. Within the insula of our patients, we analyzed data recorded at 17 contacts in the PLG (9 in the left and 8 in the right hemisphere), 32 in the ALG (16 in the left and 16 in the right hemisphere), 12 in the PSG (3 in the left and 9 in the right hemisphere), 14 in the MSG (5 in the left and 9 in the right hemisphere) and 7 in the ASG (1 in the left and 6 in the right hemisphere) (Fig. 1). After having checked for each insular gyrus that amplitudes and latencies of the laser evoked potentials were not different in the right and left hemispheres, the left contact coordinates were flipped to the right for illustration purposes. Amplitudes and latencies of responses obtained on all of the 82 electrodes were pooled together independently of their implantation side for statistical analyses.

Because of the trajectory of electrodes—perpendicular to the mid-sagittal plane—it was possible to record the activity in the opercular cortices overlying the insula. As expected, LEP latencies in the fronto-parietal opercular cortex were shorter than those of insular LEPs (97.7 ± 36.4 ms for the negative component; 149.4 ± 42 ms for the positive component). Furthermore we could check that LEP polarity reversals in the insula were not volume conducted from adjacent opercular sources (Fig. 2).

Stimulation Procedure, Recording, and Signal Averaging

LEP recordings were performed between 10 and 15 days after electrode implantation. During the recordings, the patients lay down on a bed in a quiet room.

Nociceptive Stimulation and LEPs

LEPs were recorded in response to nociceptive stimuli applied with a Nd:YAP laser (Yttrium Aluminium Perovskite; wavelength 1.34 μm, El-En®), which delivered brief radiant heat pulses of 5-ms duration. The laser beam was transmitted from the generator to the stimulating probe via an optical fiber of 10 m length. Two separate runs of 12–15 stimulations applied to the skin in the superficial radial nerve territory on the dorsum of the hand were delivered contralateral to the implanted electrodes. The inter-stimulus interval varied randomly between 10 and 25 s. The laser beam was slightly moved between two successive stimuli to avoid habituation and especially peripheral nociceptor fatigue [Greffrath et al., 2007; Schwarz et al., 2000]. The intensity used for LEP recordings was set at the beginning of the recording session according to subjects' subjective reports, rated on a visual numerical scale.

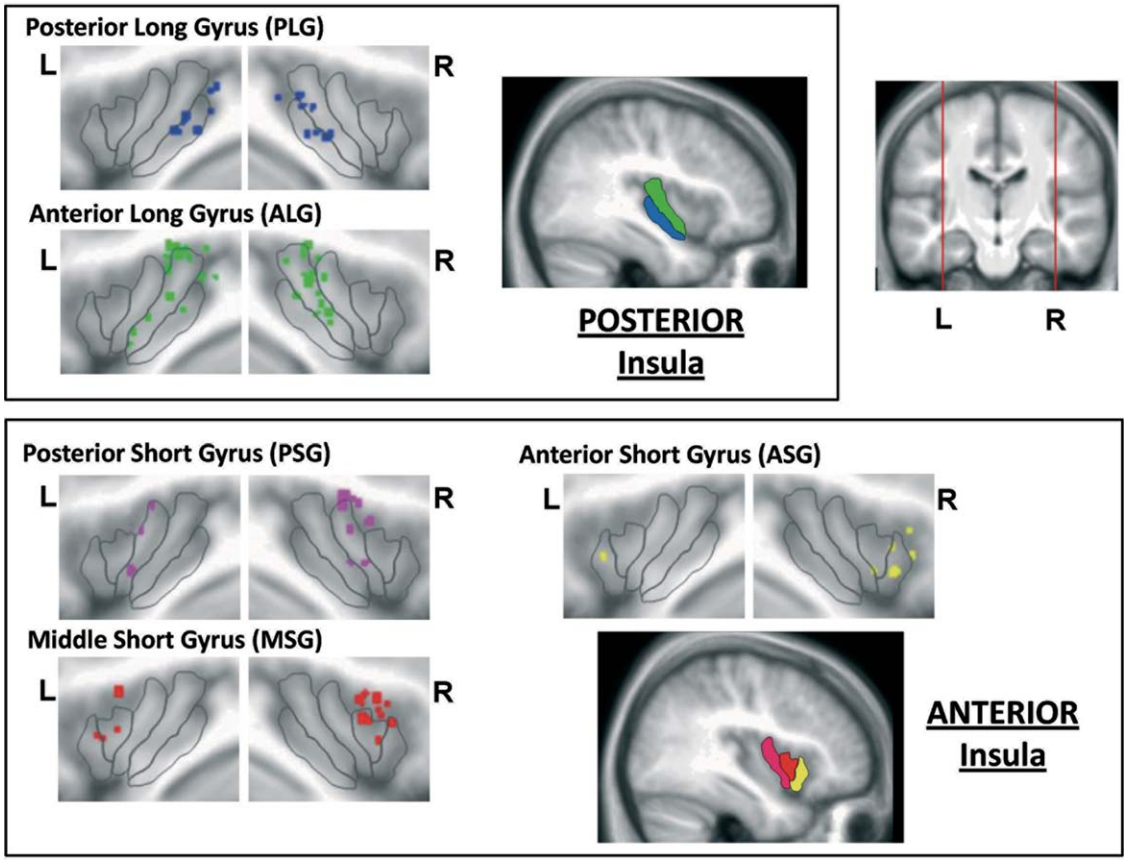

Figure 1.

Insular contacts ($n = 82$) plotted on the mean image of the 40 patients of the study. The insula is divided into a posterior part composed of two long gyri (blue and green) and an anterior part composed of three short gyri (pink, red, and yellow). Contacts are plotted according to their *y* and *z* MNI coordinates in corresponding insular gyri in the left (L) and right (R) hemispheres. Outlines of insular sulci are drawn on the patients' average MRI, explaining why some contacts do not strictly match the insular limits. The precise location of all these contacts was verified by plotting them on the corresponding MRI slices of each patient.

The printed scales consisted of 10-cm horizontal lines where the left extreme was labelled "no sensation" and the right extreme "maximal pain," with level 4 corresponding to pain threshold. During the whole recording session stimulation, intensity was kept stable at 20% above the pain threshold as measured for any given patient. The subjects had to provide pain ratings after each run of stimulation. For all patients, pain thresholds were obtained with a beam diameter of 4–5 mm and beam energy of 50–79 mJ/mm^2, very similar to the settings found in previous

TABLE I. Mean Talairach and MNI coordinates of insular contacts (±1 SD)

	Insular Gyri									
	PLG (17 contacts)		ALG (32 contacts)		PSG (12 contacts)		MSG (14 contacts)		ASG (7 contacts)	
	Tal	MNI	Tal	MNI	Tal	MNI	Tal	MNI	Tal	MNI
X (mm)	34 ± 3	38 ± 3	35 ± 3	37 ± 3	34 ± 3	37 ± 2	32 ± 3	35 ± 2	34 ± 3	37 ± 3
Y (mm)	−16 ± 7	−14 ± 7	−13 ± 8	−9 ± 7	−2 ± 4	3 ± 4	7 ± 5	11 ± 5	15 ± 9	16 ± 6
Z (mm)	1 ± 5	−1 ± 6	10 ± 8	9 ± 10	10 ± 8	8 ± 9	10 ± 4	6 ± 5	1 ± 5	−4 ± 4

PLG, posterior long gyrus; ALG, anterior long gyrus; PSG, posterior short gyrus; MSG, middle short gyrus; ASG, anterior short gyrus.

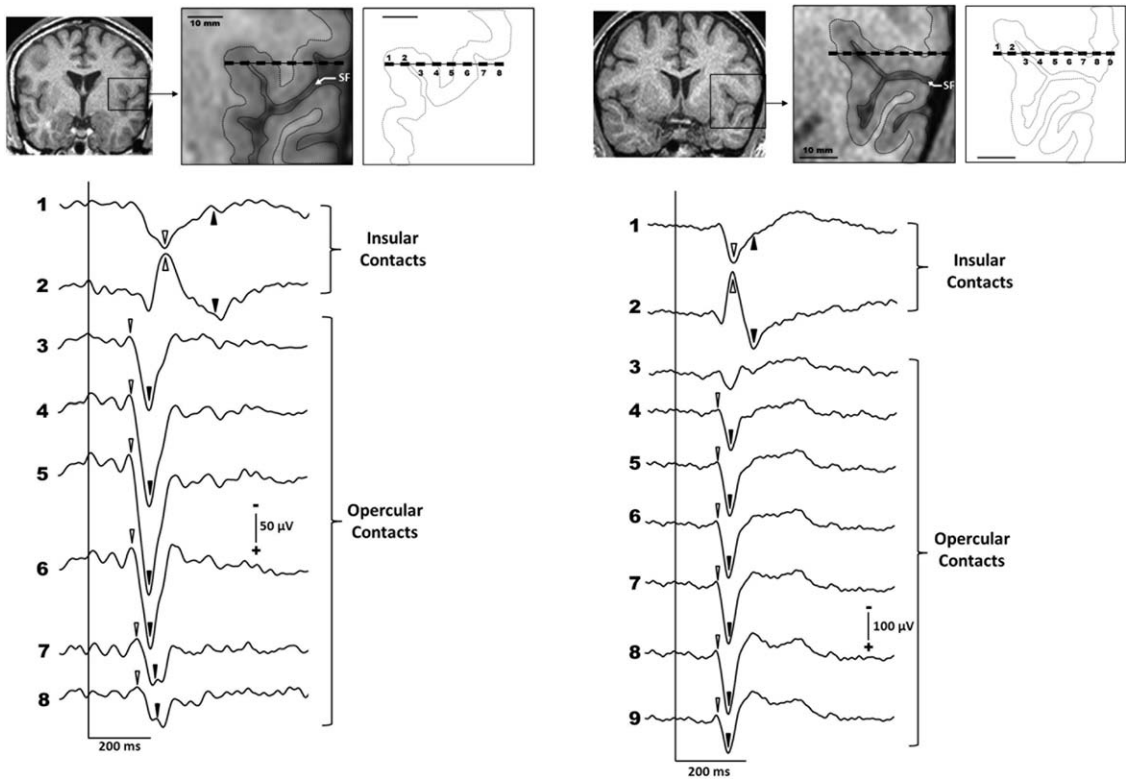

Figure 2.

Contralateral LEPs recorded along the entire trajectory of an electrode exploring both the insular and the opercular cortices in two patients (referential recordings). The electrodes were plotted on the MRI coronal slices of each patient. Apart from the latency shift between opercular and insular responses, note the polarity reversal between the two adjacent insular contacts. Both observations are in favor of distinct LEP sources in insular and opercular cortices. SF, Sylvian Fissure; White triangles, N components of the insular and opercular LEPs; Black triangles, P components of the insular and opercular LEPs.

works [Leandri et al., 2006; Perchet et al., 2008]. The mean pain intensity rating was 5.5 ± 1.4, described as "painful but tolerable" by all patients.

On-line recordings were performed using a sampling frequency of 256 Hz and a band pass filter of (−3 dB) 0.03–100 Hz using a Micromed® system.

In all patients the reference was the most superficial contact along an electrode track situated at distance of the insular region and was located in the skull outside the cortex. The reference contact was thus chosen individually according to the implantation scheme, which itself depended upon the suspected location of the epileptogenic area as determined by preimplantation data from non-invasive scalp recordings and neuroimaging data.

Data Analysis

Epoching and averaging of the EEG activity were performed off-line using Neuroscan® software. For the LEP analysis each epoch started 100 ms before and ended 900 ms after the stimulus. A prestimulus baseline correction was performed before averaging. Epochs with epileptic paroxysmal activity were rejected from analysis. Averaging was performed to reduce the background EEG noise so as to facilitate analysis of stimulus-locked activity (evoked potentials). Finally, the two runs of laser stimulation were pooled after having checked that the averaged waveforms were reproducible. For illustration purposes, we performed grand averages of LEPs recorded in each insular gyrus; however, all statistical analyses were based on amplitudes and latencies measured in each patient in referential recordings.

The different LEP components were identified according to their polarities and peak latencies using guidelines recommended by the International Federation of Clinical Neurophysiology [Cruccu et al., 2008]. Recordings in both referential and bipolar montages were considered. In the text and tables, latencies and amplitudes are given as means ± 1 SD. Amplitudes of LEPs were measured peak to peak between the first negativity and the following positive component of the response on the contact exhibiting the largest peak-to-peak response in referential mode.

TABLE II. Mean latencies and amplitudes of insular LEPs (± 1 SD)

		Latencies (ms)		Amplitudes (μV)
		N	*P*	*N-P*
Insular Gyri	PLG	220.9 ± 27.8	332.4 ± 35.6	90.7 ± 60
	ALG	212 ± 28.4	330.1 ± 31	122.7 ± 58
	PSG	237.2 ± 18.7	360.8 ± 30.3	68.2 ± 44.6
	MSG	255.8 ± 37.2	377.8 ± 49.7	51.9 ± 26.6
	ASG	309.3 ± 48.4	404.3 ± 55.8	36.2 ± 19.5

PLG, posterior long gyrus; ALG, anterior long gyrus; PSG, posterior short gyrus; MSG, middle short gyrus; ASG, anterior short gyrus.

RESULTS

Latencies and Voltages of the Insular LEPs Versus Anatomical Insular Subdivisions

Contralateral LEPs could be recorded between 100 and 500 ms after the stimulus from contacts located in all of the implanted insular gyri (Fig. 2 and Table II). They consisted of two components, a first negative wave (N) followed by a positive wave (P), as described in our previous papers [Frot and Mauguière, 2003; Frot et al., 2007, 2012]. This basic LEP morphology was identical across the whole antero-posterior extent of the insular cortex; however, the latencies and amplitudes of the responses differed according to the insular recording sites (Fig. 3).

There was a significant effect of the insular gyrus explored on the latencies of the LEPs' negative and positive components (one way ANOVA; F (4, 87) = 20, $P < 0.0001$ for N; F (4, 87) = 9.4, $P < 0.0001$ for P). The longest LEP latencies were measured in the ASG of the anterior insula (post-hoc Tukey test, $P < 0.05$), and the shortest in the ALG of the posterior insula (post-hoc Tukey test, $P < 0.05$) (Fig. 3, Table I and Supporting Information).

Concerning the EP voltages, there was also a significant effect of the insular gyrus explored on the peak to peak *N-P* amplitudes (one-way ANOVA; F (4, 87) = 8.5, $P < 0.0001$). The largest LEP amplitudes were recorded in the ALG of the posterior insula (post-hoc Tukey test,

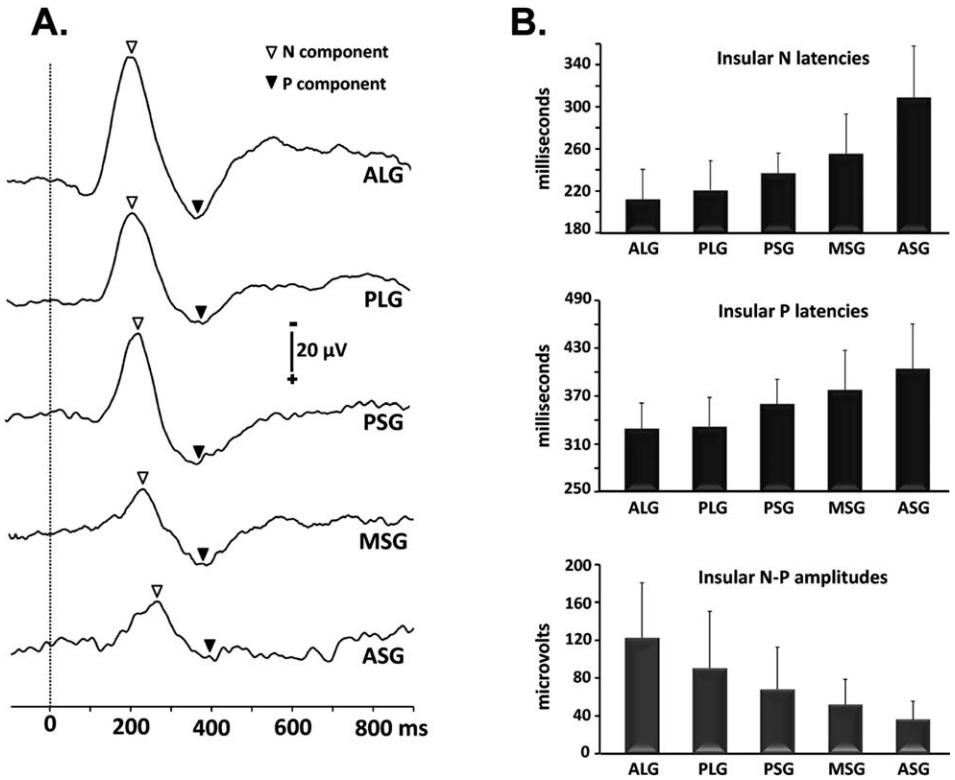

Figure 3.

A: Grand averages of contralateral LEPs recorded in the different insular gyri (referential recordings). ALG, anterior long gyrus; PLG, posterior long gyrus; PSG, posterior short gyrus; MSG, middle short gyrus; ASG, anterior short gyrus; White triangles, negative LEP components; Black triangles, positive LEP components. **B:** Histograms showing peak latencies and peak-to-peak (*N-P*) amplitudes values of LEPs recorded in the different insular gyri. Errors bars: ± 1 SD. For results of statistical analyses performed on these data see Supporting Information.

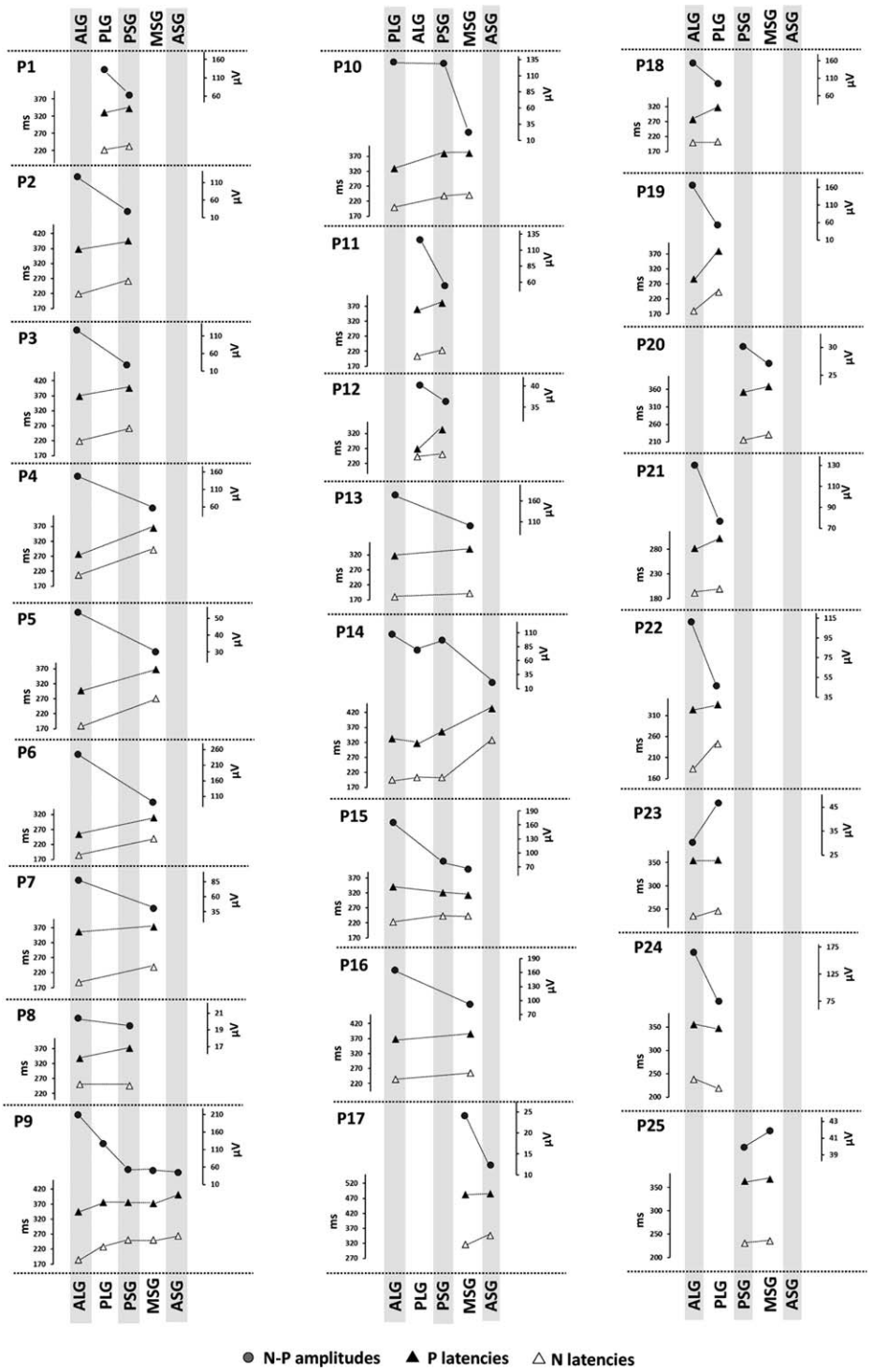

Figure 4.

Distribution of LEPs peak latencies and voltages according to the recording site inside the insula in all of the 25 subjects in whom several electrodes explored different insular gyri. Gray circles, *N-P* LEPs amplitudes; White triangles, *N* LEPs latencies; Black triangles, *P* LEP latencies. P, patient; ALG, anterior long gyrus; PLG, posterior long gyrus; PSG, posterior short gyrus; MSG, middle short gyrus; ASG, anterior short gyrus.

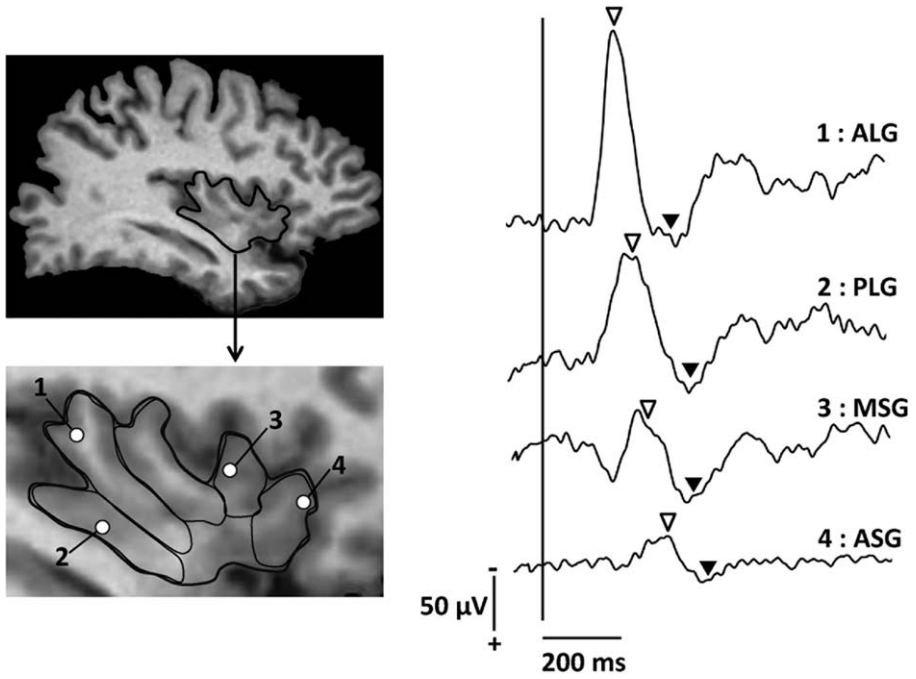

Figure 5.
Contralateral LEPs recorded in four insular gyri of one patient (referential recordings). The contacts are represented on the patient's MRI. White triangles, negative LEP components; Black triangles, positive LEP components. ALG, anterior long gyrus; PLG, posterior long gyrus; MSG, middle short gyrus; ASG, anterior short gyrus.

$P < 0.01$), and the smallest in the more anterior insular gyri (MSG and ASG) (post-hoc Tukey tests, $P < 0.05$) (Fig. 3, Table II and Supporting Information).

This group distribution of LEP latencies and voltages according to the recording site inside the insula was reproducible individually in all of the 25 subjects in whom several electrodes explored different insular gyri (see Fig. 4). An example of one patient with four electrodes implanted in four different insular gyri is illustrated in Figure 5.

Latencies and Voltages of the Insular LEPs Versus Stereotactic Coordinates of Recording Contacts

The insular LEPs were recorded at contacts located in the insular cortex between coronal planes 23 mm anterior and 27 mm posterior to the anterior commissure vertical plane (VAC – y direction); between horizontal planes at 13 mm below and 21 mm above the horizontal anterior commissure—posterior commissure plane (AC-PC – z direction); and between 32 and 43 mm from the midsagittal vertical plane (x direction). Plotting LEP amplitudes and latencies according to the y stereotactic coordinates of recording contacts, as illustrated in Figure 6, shows significant correlations between variables ($R^2 = 0.25$, F (1, 80) = 26.7, $P < 0.0001$ for N latencies, $R^2 = 0.25$, F (1, 80) = 27.06, $P < 0.0001$ for P latencies, $R^2 = 0.29$, F (1, 80) = 32.5, $P < 0.0001$ for N-P amplitudes). These data show that the more posterior the insular contact the higher the LEP amplitude and the shorter its latency.

Localization of the Insular LEP Sources

By analyzing the totality of the LEPs recorded at the 239 insular recording sites we were able, in each individual, to record an evoked response on several contiguous contacts along the same electrode track exploring from surface to depth the cortex of a single insular region and thus to look for N-P phase reversals. We observed a polarity reversal of the insular LEPs in 44% of referential and 34% of bipolar recordings along insular electrode tracks; no phase reversal was observed along 22% of electrode tracks (Fig. 7).

We recorded phase reversals of LEPs in all insular gyri. However, as illustrated in Figure 7, phase reversals were not evenly distributed across posterior and anterior insular regions and were more frequently observed in PLG and ALG (Chi-square = 24.43, df = 2, $P < 0.0001$).

We verified that the distribution of LEP latencies and voltages according to the location of recording sites (see above)

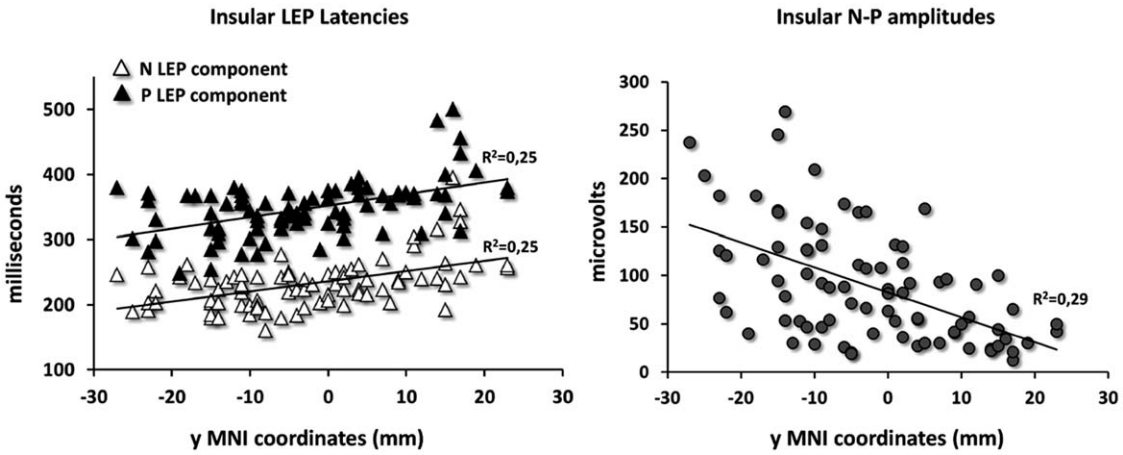

Figure 6.

Plotting of LEP peak latencies and peak-to-peak (*N-P*) amplitudes according to the *y* stereotactic coordinates (MNI space) of insular recording contacts. A linear fit is applied to each graph for LEP amplitudes (gray circles), negative (white triangles), and positive (black triangles) peak latencies. R^2 is the regression coefficient.

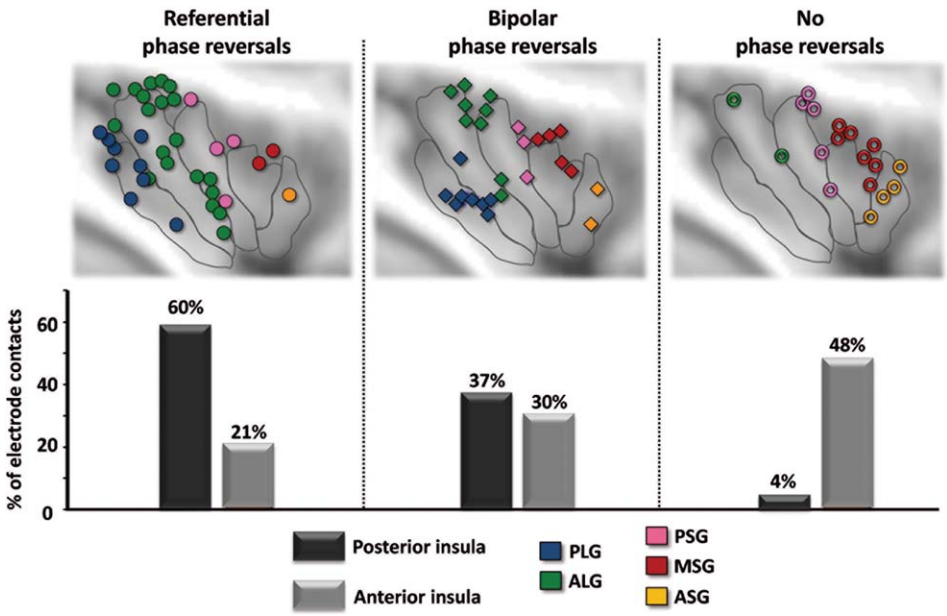

Figure 7.

The color code for contacts is the same as in Figure 1 and refers to their location in the insula. The shapes used for these contacts denote the type of LEP phase reversal observed. Circles: contacts where LEPs showed polarity reversal in referential recordings. Diamonds: contacts where LEPs showed polarity reversal in bipolar recordings. Rings: contacts showing no polarity reversals. Outlines of insular sulci are drawn on the patients' average MRI, explaining why some contacts do not strictly match the insular limits. The precise location of all these contacts was verified by plotting them on the corresponding MRI slices of each patient. The histograms represent the percentage of contacts recording phase reversals in referential and bipolar recordings or no phase reversals according to the contact location (posterior vs. anterior insula in dark and light gray, respectively). PLG, posterior long gyrus; ALG, anterior long gyrus; PSG, posterior short gyrus; MSG, middle short gyrus; ASG, anterior short gyrus.

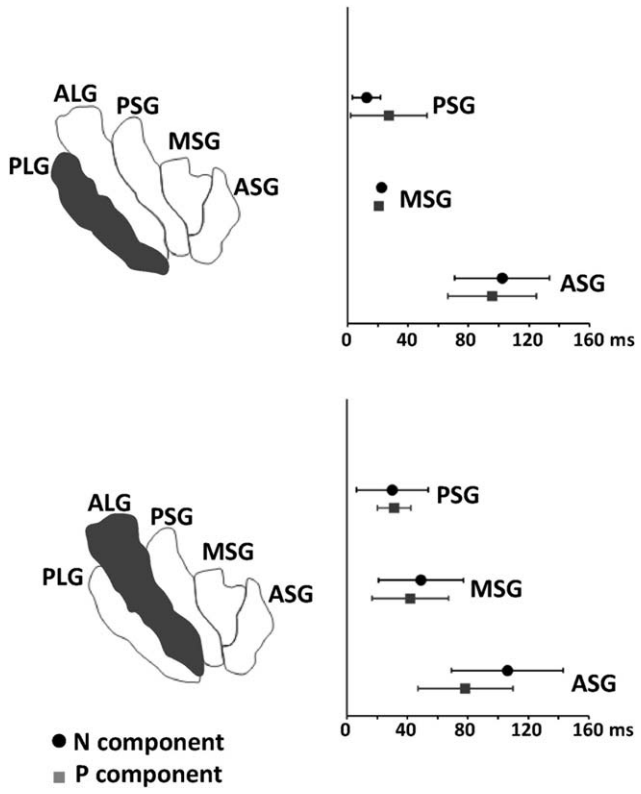

Figure 8.

Upper panel: Plot of the latency delays between the PLG and the three anterior insular gyri (PSG, MSG, ASG) for the negative (black circle) and the positive (gray square) components of the LEPs. Lower panel: Plot of the latency delays between the ALG and the three anterior insular gyri (PSG, MSG, ASG) for the negative (black circle) and the positive (gray square) LEP components. Errors bars: ± 1 SD.

was unchanged when only those 78% of electrode tracks showing a phase reversal of LEPs were included in the group study.

DISCUSSION

Brain imaging studies have shown that pain is the stimulus that activates the largest area in the insular cortex [Kurth et al., 2010a], extended to all of its cytoarchitectonic subdivisions [Mazzola et al., 2012a]. By using intra-cerebral recordings in this study, we were able to show a spatial and temporal gradient of pain responses from the upper posterior to the lower anterior insular cortex. Nociceptive responses in the posterior part of the insula were recorded with the shortest latencies and the highest amplitudes whereas they peaked later and with smaller voltages in the anterior insular cortex. Three questions arise from our findings: (i) Are LEPs recorded in posterior and anterior insula generated by separate sources? (ii) What is the substratum of the latency delay between posterior and anterior insular LEPs? (iii) How might the functional dichotomy suggested by the spatio-temporal gradient of insular LEPs relate to the cytoarchitecture and connectivity of the insular cortex?

Distinct Sources for Insular LEPs With Distinct Latencies

The question whether the spatio-temporal gradient of pain responses reflects activation of distinct sources in the posterior and anterior parts of the insula is addressed by the surface-to-depth phase reversals of the LEPs that we observed in all insular gyri along electrode tracks oriented perpendicular to the insular surface (see Fig. 7), favoring the hypothesis of distinct and sequentially activated generators. A phase reversal of LEPs recorded by a pair of contacts separated by a distance of only 1.5 mm is likely to be close to the source of the signal. For phase reversals observed in referential recordings one can even assume that the LEP dipolar source is oriented parallel to the electrode track, while this is not possible for phase reversals in bipolar recordings. It is noteworthy that LEP phase reversals were less frequent in the anterior part of the insula, an observation which may reflect the fact that the insular cytoarchitecture is characterized by a progressively decreasing density and thickness of granular Layers II and IV from upper posterior to lower anterior insular cortex [Morel et al., 2013].

Substratum of the Latency Delay Between Posterior and Anterior Insular LEPs

We observed latency delay between responses recorded in PLG and ALG posterior to the insular central sulcus and those recorded in PSG and MSG, located anterior to the central sulcus. Figure 8 shows the LEP latency shifts between post-central (PLG, ALG) and precentral (PSG, MSG, ASG) insular gyri measured in patients with at least one contact caudal and rostral to the central sulcus. Within each of these pairs of areas there was no significant difference in LEP latencies, whereas LEPs consistently peaked with a longer latency anterior to the central sulcus (see Supporting Information). The range of latency differences was 12.4 ± 9 ms (PLG vs. PSG) to 48.9 ± 28 ms (ALG vs. MSG), similar to the 26–28 ms recently measured by Almashaikhi et al. (2013) for evoked potentials recorded after direct insular stimulation, thus suggesting input transmission through mono- or polysynaptic pathways inside the insular cortex. The LEP latency shift between postcentral insular cortex and the most anterior insular gyrus (ASG) was much longer (around 100 ms; see Fig. 8) and does not match with that evaluated by intra-insular evoked potentials [Almashaikhi et al., 2013]. There is no clear evidence of direct connections between the more posterior granular subdivisions of the insula and the anterobasal agranular sector [Augustine et al., 1996; Friedman et al., 1986; Mufson and Mesulam, 1982], which was not explored by

Almashaikhi et al. [2013]. The delay of ~100 ms observed between the shortest LEP latencies recorded in the long anterior gyrus of the posterior insula and the longest latencies measured in the most anterior insular gyrus (ASG) argues against propagation through direct connections. This delay rather suggests a postero-anterior sequential processing of pain input through multisynaptic pathways within the insular cortex. The alternative hypothesis would be that the different parts of the insular cortex could be activated by pain input via distinct thalamocortical fibers with different conduction velocities (e.g., slower for those targeting the anterior insula) but, to our knowledge, this is not supported by any anatomical or electrophysiological data.

Functional Dichotomy Revealed by LEPs Versus Cytoarchitecture and Connectivity of the Insular Cortex

Nociceptive responses obtained in this study were localized in the posterior or in the anterior insula according to their positioning caudal or rostral to the central sulcus, and more precisely in each insular gyrus. It is well known that the insula's anatomical macroscopic subdivision does not match its cytoarchitectonic organization [Morel et al., 2013; Nieuwenhuys, 2012]. A probabilistic stereotactic atlas was presented by Kurth et al. [2010b] in which part of the posterior insular cortex and the adjacent opercular regions were divided into distinct cytoarchitectonic zones. For 63% of our posterior insular electrode contacts, the corresponding cytoarchitectonic subdivision could be determined with reference to the atlas by Kurth et al. [2010b]. 37% were located in granular areas (25% in Ig2; 12% in Ig1) and 4% in the dysgranular part (Id1). It is noteworthy that when plotted according to the stereotactic MNI coordinates delineating the borders of cytoarchitectonic subdivisions in this probabilistic atlas (using the SPM Anatomy Toolbox, Eickhoff et al., 2005), 22% of our posterior insula contacts, whose positions in the insular cortex were individually confirmed by plotting them on the appropriate MRI slices of each patient, were located in the opercular region OP3 [Eickhoff et al., 2010], neighboring the upper part of Ig2 region. Interindividual variation of the border between OP3 and Ig2 regions in our 40 patients is likely to account for this discrepancy between insular localization based on probabilistic cytoarchitectonic maps drawn by Kurth et al. [2010b] in 10 subjects versus those that we determined individually. Moreover, our finding that LEPs recorded at insular sites peaked with a longer latency than that of LEPs recorded at adjacent opercular sites in our patients, as previously observed [Frot and Mauguière, 2003], confirms the insular localization of our recording contacts (see Fig. 2). Stereotactic coordinates of the remaining 37% of contacts located caudal to the central sulcus and those of all contacts located in the anterior insula were anterior to the insular cytoarchitectonic subdivisions mapped by Kurth et al. [2010b]. When plotting the locations of these contacts in the MRI-registered cytoarchitectonic maps recently drawn by Morel et al. [2013] in four specimens obtained from post mortem brains, it appears that they were distributed from the dysgranular subdivisions (Id3, Id2, Id1) to the agranular zones for the more anterior contacts (Ia2).

The temporal gradient that we observed between LEPs recorded posterior and anterior to the central sulcus of the insula suggests a functional duality of the insular cortex regarding its role in pain input processing. The clustering of LEP latencies in two regions separated by the central sulcus is in line with recent studies on anatomical and functional insular connectivity based on MR probabilistic tractography [Cerliani et al., 2012; Cloutman et al., 2012] and fMRI BOLD fluctuations in the resting brain [Cauda et al., 2011]. The two approaches converge on a clear bipartition of the insula with different connectivity patterns that could underlie different functions. They showed that the anterior insula is connected to the anterior cingulate cortex and limbic regions involved in emotions while the middle-posterior insula is connected to premotor, sensorimotor, and mid-posterior cingulate cortices suggesting a role in sensorimotor integration.

Regarding the role of the insular cortex in the processing of pain input, the concept of a functional duality is commonly accepted. Insular LEP recordings [Frot and Mauguière, 2003; Frot et al., 2007] and studies of pain responses to insular cortex stimulation [Mazzola et al., 2006, 2012b; Ostrowsky et al., 2002] have shown that posterior insular cortex is involved mostly in the coding of pain intensity with a blurred somatotopic representation of the skin surface. Conversely, the anterior insula, which plays a central role in mediating interoceptive awareness and the "subjective experience of feelings" [Craig, 2002], is involved in viscero-autonomic functions, affective reaction to pain [Augustine, 1996; Mesulam and Mufson, 1985; Nieuwenhuys, 2012] including empathic feeling of the pain of others [Corradi-Dell'acqua et al., 2011; Jackson et al., 2005; Singer et al., 2004], and in pain modulation by emotions [Stancak and Fallon, 2013; Stancak et al., 2013; Wiech and Tracey, 2009]. Our study shows that both of these insular sub-areas, in spite of their different implication in the processing of pain input, do respond to a peripheral pain stimulus within a 200–400 ms latency range but also that this pain response occurs first, and is of larger amplitude, in the posterior insula.

Sources activated with the shortest latencies were located in the long anterior gyrus of the posterior insula suggesting that spino-thalamic inputs may be directly transmitted from subcortical structures to this insular gyrus. This assumption is coherent with anatomical studies in primates showing that the thalamic posterior supragenicular complex including the posterior portion of the ventral medial nucleus (VMPo), which nociceptive and thermoreceptive spinothalamic afferent fibers target [Craig et al., 1994; Dum et al., 2009], projects to the

postero-superior granular part of the insular cortex [Dum et al., 2009]. LEP sources in this posterior part of the insula could also be activated through cortico-cortical connections by input transmitted from somatosensory cortices (S1 and S2), which are activated about 70–80 ms before the insula by nociceptive stimuli during intracranial recordings [Frot and Mauguière, 2003; Frot et al., 2012]. In primates, the posterior insula is reciprocally connected with the neighboring secondary somatosensory cortex and receives projections from the primary somatosensory cortex and somatosensory association areas [Augustine 1996; Friedman et al., 1986; Mesulam and Mufson, 1985; Mufson and Mesulam, 1982]. In humans, a recent study using in vivo MRI probabilistic tractography to map the structural connectivity of insular subregions showed that only the more posterior insular gyri are connected to the post-central cortex (including S1), the fronto-parietal operculum including S2, and the motor cortex [Cloutman et al., 2012].

Involvement of the posterior insula in nociception is coherent with numerous neuroimaging studies showing its role in sensory aspects of pain processing [for a review, see Kurth et al., 2010a]. By comparing fMRI activations related to the coding of physical stimulus intensity with those occurring exclusively when the stimulus is perceived as painful, Oertel et al. [2012] suggested that the posterior insula is part of a cortical network specifically devoted to the perception of pain. Last, the posterior insula is one of the two cortical regions (the other being the secondary somatosensory cortex) where direct electrical stimulations can provoke pain sensations [Ostrowsky et al., 2000, 2002; Mazzola et al., 2006, 2012b]. Our findings raise the question whether anterior and posterior insular LEPs correlate differently with pain intensity ratings, which could be addressed in a further study by averaging responses according to the pain rating of each stimulus.

Our findings suggest a transfer of nociceptive information from posterior to anterior insula. It is noteworthy that very dense intra-insular connections [Augustine et al., 1996] could convey this nociceptive information from posterior to anterior insula, especially between the granular and dysgranular parts of the insular cortex [Mufson and Mesulam, 1982]. While autoradiographic studies in monkeys suggested that, although bidirectional, the majority of intra-insular connections were from anterior to posterior insular regions [Mesulam and Mufson, 1982; Seltzer and Pandya, 1991], electrophysiology recently showed that most of the intra-insular connections are reciprocal in humans [Almashaikhi et al., 2013].

The postero–anterior direction of the nociceptive information flux within the insula is likely to reflect the integrative functional role of this cortical region in pain processing. This is in line with recent data obtained with in vivo MRI probabilistic tractography in humans showing that the trajectory of connections is gradually organized along the rostrocaudal axis of the insula, spanning from the most anterior insular territory in the ASG to the posterior insular region in the dorsal PLG [Cerliani et al., 2012]. These data suggest a relationship between topographical variation of connectivity patterns and the organization of insular cytoarchitecture, the anterior agranular insula having the highest connection probability with limbic regions and the more posterior granular and dysgranular insular cortex being highly connected with posterior parietal and somatosensory regions [Cerliani et al., 2012].

Overall, our findings suggest that painful input is first processed in the posterior insula, where it is known to be coded in terms of intensity and anatomical location, and conveyed to the anterior insula, where the emotional reaction to pain is elaborated.

ACKNOWLEDGMENTS

The authors thank Dr M. Guenot (Department of Functional Neurosurgery) for stereotactic electrode implantation and Drs J. Isnard and P. Ryvlin for the opportunity to study their patients. The authors are grateful to Claire Bradley and Alexander Hammers for carefully revising the manuscript. The authors declare no conflicts of interest.

REFERENCES

Almashaikhi T, Rheims S, Ostrowsky-Coste K, Montavont A, Jung J, De Bellescize J, Arzimanoglou A, Keo Kosal P, Guénot M, Bertrand O, Ryvlin P (2013): Intrainsular functional connectivity in human. Hum Brain Mapp. doi: 10.1002/hbm.22366.

Apkarian AV, Bushnell MC, Treede RD, Zubieta JK (2005): Human brain mechanisms of pain perception and regulation in health and disease. Eur J Pain 9:463–484.

Ashburner J, Friston KJ (2005): Unified segmentation. Neuroimage 26:839–851.

Augustine JR (1996) Circuitry and functional aspects of the insular lobe in primates including humans. Brain Res Brain Res Rev 22:229–244.

Berthier M, Starkstein S, Leiguarda R (1988) Asymbolia for pain: A sensory-limbic disconnection syndrome. Ann Neurol 24:41–49.

Brett M, Anton JL, Valabregue R, Poline JB (2002): Region of interest analysis using an SPM toolbox [abstract] Presented at the 8th International Conference on Functional Mapping of the Human Brain, June 2–6, 2002, Sendai, Japan.

Brooks JC, Zambreanu L, Godinez A, Craig AD, Tracey I (2005): Somatotopic organisation of the human insula to painful heat studied with high resolution functional imaging. Neuroimage 27: 201–209.

Cauda F, D'Agata F, Sacco K, Duca S, Geminiani G, Vercelli A (2011): Functional connectivity of the insula in the resting brain. Neuroimage 55:8–23.

Cerliani L, Thomas RM, Jbabdi S, Siero JC, Nanetti L, Crippa A, Gazzola V, D'Arceuil H, Keysers C (2012): Probabilistic tractography recovers a rostrocaudal trajectory of connectivity variability in the human insular cortex. Hum Brain Mapp 33: 2005–2034.

Cloutman LL, Binney RJ, Drakesmith M, Parker GJ, Lambon Ralph MA (2012) The variation of function across the human insula mirrors its patterns of structural connectivity: Evidence from in vivo probabilistic tractography. Neuroimage 59:3514–3521.

Corradi-Dell'Acqua C, Hofstetter C, Vuilleumier P (2011): Felt and seen pain evoke the same local patterns of cortical activity in insular and cingulate cortex. J Neurosci 31:17996–18006.

Craig AD (2002): How do you feel? Interoception: The sense of the physiological condition of the body. Nat Rev Neurosci 3: 655–666.

Craig AD, Bushnell MC, Zhang ET, Blomqvist A (1994): A thalamic nucleus specific for pain and temperature sensation. Nature 372:770–773.

Cruccu G, Aminoff MJ, Curio G, Guerit JM, Kakigi R, Mauguière F, Rossini PM, Treede RD, Garcia-Larrea L (2008) Recommendations for the clinical use of somatosensory-evoked potentials. Clin Neurophysiol 119:1705–1719.

Duerden EG, Albanese MC (2011) Localization of pain-related brain activation: A meta-analysis of neuroimaging data. Hum Brain Mapp 34:109–149.

Dum RP, Levinthal DJ, Strick PL (2009) The spinothalamic system targets motor and sensory areas in the cerebral cortex of monkeys. J Neurosci 29:14223–14235.

Eickoff SB, Stephan KE, Mohlberg H, Grefkes C, Fink GR, Amunts K, Zilles K (2005) A new SPM toolbox for combining probabilistic cytoarchitectonic maps and functional imaging data. Neuroimage 25:1325–1335.

Eickhoff SB, Heim S, Zilles K, Amunts K (2006): Testing anatomically specified hypotheses in functional imaging using cytoarchitectonic maps. NeuroImage 32:570–582.

Eickhoff SB, Jbabdi S, Caspers S, Laird AR, Fox PT, Zilles K, Behrens TEJ (2010): Anatomical and functional connectivity of cytoarchitectonic areas within the human parietal operculum. J Neurosci 30:6409–6421.

Friedman DP, Murray EA, O'Neill JB, Mishkin M (1986): Cortical connections of the somatosensory fields of the lateral sulcus of macaques: Evidence for a corticolimbic pathway for touch. J Comp Neurol 252:323–347.

Frot M, Mauguière F (2003): Dual representation of pain in the operculo-insular cortex in humans. Brain 126:438–450.

Frot M, Magnin M, Mauguière F, Garcia-Larrea L (2007): Human SII and insula differently encode thermal stimuli. Cereb Cortex 17:610–620.

Frot M, Magnin M, Mauguière F, Garcia-Larrea L (2012): Cortical representation of pain in primary sensory-motor areas (S1/M1)-a study using intracortical recordings in humans. Hum Brain Mapp Jun 15. doi: 10.1002/hbm.22097

Garcia-Larrea L, Peyron R (2013): Pain matrices and neuropathic pain matrices: A review. Pain 154 (Suppl 1):S29–S43. doi: 10.1016/j.pain.2013.09.001.

Garcia-Larrea L, Frot M, Valeriani M (2003) Brain generators of laser-evoked potentials: From dipoles to functional significance. Neurophysiol Clin 33:279–292.

Garcia-Larrea L, Perchet C, Creac'h C, Convers P, Peyron R, Laurent B, Mauguière F, Magnin M (2010): Operculo-insular pain (parasylvian pain): A distinct central pain syndrome. Brain 133:2528–2539.

Greffrath W, Baumgärtner U, Treede RD (2007): Peripheral and central components of habituation of heat pain perception and evoked potentials in humans. Pain 132:301–311.

Henderson LA, Gandevia SC, Macefield VG (2007): Somatotopic organization of the processing of muscle and cutaneous pain in the left and right insula cortex: A single-trial fMRI study. Pain 128:20–30.

Isnard J, Guénot M, Ostrowsky K, Sindou M, Mauguière F (2000): The role of the insular cortex in temporal lobe epilepsy. Ann Neurol 48:614–623.

Isnard J, Guénot M, Sindou M, Mauguière F (2004) Clinical manifestations of insular lobe seizures: A stereo electroencephalographic study. Epilepsia 45:1079–1090.

Jackson PL, Meltzoff AN, Decety J (2005): How do we perceive the pain of others? A window into the neural processes involved in empathy. Neuroimage 24:771–779.

Kurth F, Zilles K, Fox PT, Laird AR, Eickhoff SB (2010a): A link between the systems: Functional differentiation and integration within the human insula revealed by meta-analysis. Brain Struct Funct 214(5-6):519–534.

Kurth F, Eickhoff SB, Schleicher A, Hoemke L, Zilles K, Amunts K (2010b): Cytoarchitecture and probabilistic maps of the human posterior insular cortex. Cereb Cortex 20:1448–1461.

Leandri M, Saturno M, Spadavecchia L, Iannetti GD, Cruccu G, Truini A (2006): Measurement of skin temperature after infrared laser stimulation. Neurophysiol Clin 36:207–218.

Mazzola L, Isnard J, Mauguière F (2006): Somatosensory and pain responses to stimulation of the second somatosensory area (SII) in humans. A comparison with SI and insular responses. Cereb Cortex 16:960–968.

Mazzola L, Faillenot I, Barral FG, Mauguière F, Peyron R (2012a): Spatial segregation of somato-sensory and pain activations in the human operculo-insular cortex. Neuroimage 60: 409–418.

Mazzola L, Isnard J, Peyron R, Mauguière F (2012b): Stimulation of the human cortex and the experience of pain: Wilder Penfield's observations revisited. Brain 135:631–640.

Mesulam MM, Mufson EJ (1982): Insula of the old world monkey. III. Efferent cortical output and comments on function. J Comp Neurol 212:38–52.

Mesulam MM, Mufson EJ (1985): The insula of Reil in man and monkey. In: Peters A, Jones EG, editors. Association and Auditory Cortices. New York: Plenum. pp 179–226.

Moisset X, Bouhassira D (2007): Brain imaging of neuropathic pain. Neuroimage 37 (Suppl 1):S80–S88.

Morel A, Gallay MN, Baechler A, Wyss M, Gallay DS (2013): The human insula: Architectonic organization and postmortem MRI registration. Neuroscience 236:117–135.

Mufson EJ, Mesulam MM (1982): Insula of the old world monkey. II. Afferent cortical input and comments on the claustrum. J Comp Neurol 212:23–37.

Naidich TP, Kang E, Fatterpekar GM, Delman BN, Gultekin SH, Wolfe D, Ortiz O, Yousry I, Weismann M, Yousry TA (2004): The insula: Anatomic study and MR imaging display at 1.5 T. AJNR Am J Neuroradiol 25:222–232.

Nieuwenhuys R (2012): The insular cortex: A review. Prog Brain Res 195:123–163.

Oertel BG, Preibisch C, Martin T, Walter C, Gamer M, Deichmann R, Lötsch J (2012): Separating brain processing of pain from that of stimulus intensity. Hum Brain Mapp 33:883–894.

Ostrowsky K, Isnard J, Ryvlin P, Guénot M, Fischer C, Mauguière F (2000): Functional mapping of the insular cortex: Clinical implication in temporal lobe epilepsy. Epilepsia 41:681–686.

Ostrowsky K, Magnin M, Ryvlin P, Isnard J, Guenot M, Mauguière F (2002) Representation of pain and somatic sensation in the human insula: A study of responses to direct electrical cortical stimulation. Cereb Cortex 12:376–385.

Perchet C, Godinho F, Mazza S, Frot M, Legrain V, Magnin M, Garcia-Larrea L (2008): Evoked potentials to nociceptive stimuli delivered by CO2 or Nd:YAP lasers. Clin Neurophysiol 119:2615–2622.

Rorden C, Brett M (2000): Stereotaxic display of brain lesions. Behav Neurol 12:191–200.

Schnitzler A, Ploner M (2000): Neurophysiology and functional neuroanatomy of pain perception. J Clin Neurophysiol 17: 592–603.

Schwarz S, Greffrath W, Büsselberg D, Treede RD (2000): Inactivation and tachyphylaxis of heat-evoked inward currents in nociceptive primary sensory neurones of rats. J Physiol 528: 539–549.

Schweinhardt P, Bushnell MC (2010): Pain imaging in health and disease—How far have we come? J Clin Invest 120:3788–3797.

Seltzer B, Pandya DN (1991) Post-rolandic cortical projections of the superior temporal sulcus in the rhesus monkey. J Comp Neurol 312:625–640.

Singer T, Seymour B, O'Doherty J, Kaube H, Dolan RJ, Frith CD (2004): Empathy for pain involves the affective but not sensory components of pain. Science 303:1157–1162.

Stancak A, Fallon N (2013): Emotional modulation of experimental pain: A source imaging study of laser evoked potentials. Front Hum Neurosci 7:1–16.

Stancak A, Ward H, Fallon N (2013): Modulation of pain by emotional sounds: A laser-evoked potential study. Eur J Pain 17:324–335.

Talairach J, Tournoux P (1988): Coplanar Stereotaxic Atlas of the Human Brain. 3-Dimensional Proportional System: An approach to Cerebral Imaging. Stuttgart: Georg Thieme Verlag.

Wiech K, Tracey I (2009): The influence of negative emotions on pain: Behavioral effects and neural mechanisms. Neuroimage 47:987–994.